J|A|C|S
ARTICLES
Published on Web 04/01/2004

Preparation of Protein Gradients through the Controlled Deposition of Protein−Nanoparticle Conjugates onto Functionalized Surfaces

Stephan Krämer,[†] Huan Xie,[†] John Gaff,[†] John R. Williamson,[†] Alexander G. Tkachenko,[†] Navid Nouri,[‡] David A. Feldheim,[‡] and Daniel L. Feldheim*,[†]

Contribution from the Department of Chemistry, North Carolina State University, Raleigh, North Carolina 27695, and Department of Molecular, Cellular and Developmental Biology, University of California Santa Cruz, 427 Sinsheimer Laboratories, Santa Cruz, California 95064

Received December 12, 2003; E-mail: dan_feldheim@ncsu.edu

Abstract: This paper describes a simple method for the preparation and characterization of protein density gradients on solid supports. The method employs colloidal metal nanoparticles as protein carriers and optical tags and is capable of forming linear, exponential, 1D, 2D, and multiprotein gradients of varying slope without expensive or sophisticated surface patterning techniques. Surfaces patterned with proteins using the procedures described within are shown to support cell growth and are thus suitable for studies of protein−cell interactions.

Introduction

Molecular gradients are of widespread interest in biological studies because chemical potential gradients play a key role in cell signaling and proliferation. In the mammalian brain for example, patterns of neural connections are mainly generated during embryonic development when each newly born neuron sends out an axon that contains a growth cone at its tip. Growth cones detect and respond to signaling molecules presented by cells in the environment, which in turn direct axons to their targets in a stereotyped manner.

Recent experimental work has led to the identification of many of these signaling molecules, called axon guidance molecules. These molecules can be divided into four classes based on their general mechanism of action. Some molecules work from long range, via diffusion from a point source, and act as either attractants or repellents. There are also short-range attractants and repellents. These molecules are tethered to the cell surface and act at their site of synthesis. The guidance of axons appears to involve the simultaneous operation of several, and in some cases possibly all four, of these guidance forces. Thus, an individual axon might be "pushed" from behind by a chemorepellent, and also "pulled" from afar by a chemoattractant.[1]

Often, axon guidance molecules are presented to growth cones as gradients, created by diffusion from a point source (for soluble molecules) or by patterns of gene expression (for membrane-bound molecules). Ephrins are part of a family of membrane-bound proteins implicated in axon guidance. Ephrin-A2 and ephrin-A5 are each sufficient to repel chick or mouse retinal ganglion cell (RGC) axons with a topographically specific preference for temporal axons. Ephrin-B has been shown to have attractive properties toward EphB receptor bearing axons.[1] Despite intense study, a number of key neuroscience questions about ephrins remain outstanding. For example, how are gradients of information read by axons? Are absolute levels of molecules important for axon guidance or is the slope of the gradient? How do growth cones simultaneously read multiple cues at once? These questions have motivated our groups and others to develop in vitro axon guidance assays. This has necessitated new methods for patterning and characterizing protein density gradients on solid supports.

Surface-bound molecular gradients have been reported previously. For a review of some of the techniques used for creating gradients see Ruardy et al.[2] Polymer surfaces have been modified with chemical gradients by several techniques including (i) corona discharge with gradually increasing power across the surface, (ii) plasma treatment through a shadow mask, (iii) radio frequency glow discharge through a slowly moving cover over the sample, and (iv) ion deposition with increasing current.[3] Surface-bound gradients of polymers on silica substrates have also been created by varying the contact time between a solution-phase monomer and surface-bound initiator.[4−8]

[†] North Carolina State University.
[‡] University of California Santa Cruz.

(1) (a) TessierLavigne, M.; Goodman, C. S. *Science* **1996**, *274*, 1123. (b) Cheng, H.-J.; Nakamoto, M.; et al. *Cell* **1995**, *82*, 371. (c) Feldheim, D. A.; Vanderhaeghen, P.; et al. *Neuron* **1998**, *21*, 1303.
(2) Ruardy, T. G.; Schakenraad, J. M.; vanderMei, H. C.; Busscher, H. J. *Surf. Sci. Rep.* **1997**, *29*, 3.
(3) Wijesundara, M. B. J.; Fuoco, E.; Hanley, L. *Langmuir* **2001**, *17*, 5721.
(4) Wu, T.; Efimenko, K.; Vlcek, P.; Subr, V.; Genzer, J. *Macromolecules* **2003**, *36*, 2448.
(5) Efimenko, K.; Genzer, J. *Adv. Mater.* **2001**, *13*, 1560.
(6) Genzer, J.; Fischer, D. A.; Efimenko, K. *Adv. Mater.* **2003**, *15*, 1545.
(7) Tomlinson, M. R.; Genzer, J. *Chem. Commun.* **2003**, 1350.
(8) Tomlinson, M. R.; Genzer, J. *Macromolecules* **2003**, *36*, 3449.

10.1021/ja031674n CCC: $27.50

The ability of thiol-functionalized molecules to bind to gold substrates has been exploited for the preparation of molecular gradients. The diffusion of thiols through a polysaccharide matrix and onto a gold substrate was shown to create a molecular gradient.[9−12] Morgenthaler et al. presented a simple and reproducible approach for the preparation of molecular gradients in which a gold slide was immersed into a thiol solution at a controlled rate. The subsequent immersion in a second thiol solution resulted in a two-component gradient.[13] Bohn and co-workers reported the use of a spatially varying electrochemical potential during the adsorption/desorption of alkanethiols on a gold electrode to form a thiol gradient.[14−19] Fuierer et al. used a scanning tunneling microscope to produce gradients on the nanometer scale via replacement lithography.[20]

Another class of molecules that can form monolayers on surfaces is the alkylsilanes. The diffusion of silanes in a liquid or vapor phase over glass slides results in a surface gradient. The appropriate choice of silane leaves a molecular gradient that can be further modified with metal nanoparticles or proteins.[2,4−6,21−29]

Axon guidance molecules have been attached to surfaces previously. An in vitro assay in which 90 mm wide alternating stripes of membranes from anterior and posterior optic tecta provided some of the first supporting evidence for the molecular basis of retinotectal chemoaffinity and chemorepulsion.[30,31] This type of assay is an effective "all or nothing" test for neuron−molecule compatibility. However, the test cannot provide more detailed information vis-à-vis axon guidance and the role of chemical gradients on the formation of neural topographic maps.

To address the limitations of the stripe assay, Rosentreter and co-workers developed a method for producing gradients of posterior and anterior membranes on a capillary pore filter.[32] The method used vacuum filtration and was capable of producing linear and exponential gradients of optic tecta membranes.

Whitesides has assembled gradients of laminin and bovine serum albumin (BSA) within microfluidic channels patterned into poly(dimethylsiloxane) chips.[33,34] The chip, fabricated with photolithography and microcontact printing, contained five parallel serpentine channels that merged into a single channel. BSA and laminin were combined in the serpentine channels in various proportions. The solutions flowed into the single channel under laminar flow conditions and deposited onto the floor of the channel to form a surface-bound gradient. Growth of hippocampal neural axons toward the serpentine channel with the highest initial laminin concentration was observed. The actual laminin surface concentration was not reported.[33]

The surface patterning techniques reviewed briefly above have enabled the study of axon growth in response to surface-confined molecules, thus providing important model systems of membrane-bound axon guidance proteins. Current methods of gradient fabrication are limited with respect to either the choice of substrate (filters, lithographic substrates), the ability to create gradients of varying slopes or densities, or gradient dimensionality (1D vs 2D). The methods described below do not require specialized techniques such as lithography, can be performed using any substrate material, and can be used to create defined molecular gradients of varying slopes, in 1D or 2D.

Materials and Methods

Preparation of Protein Density Gradients. General Methods. The procedure for preparing surface-bound protein density gradients is based largely upon the work of Natan and co-workers.[35] Natan's group showed that by modifying a glass substrate with cationic moieties such as alkylamines, anionic gold nanoparticles could be adsorbed from solution onto the slide. The density of nanoparticles adsorbed onto the surface was controlled simply by the length of time the slide was immersed in the nanoparticle solution. Gold nanoparticle density gradients were formed by immersing a slide in a solution of gold nanoparticles (30 nM) at a controlled rate. The side of the slide in contact with the solution the longest contained the highest density of nanoparticles. Natan used nanoparticle density gradients to determine the optimum particle density for surface-enhanced Raman spectroscopy.

To create protein gradients, colloidal metal nanoparticles (8 nm diameter silver and 12 or 20 nm gold) were first modified with a protein of interest (bovine serum albumin, ephrin-A5, ephrin-B1). A glass slide modified with cationic moieties (e.g., poly-L-lysine) was placed in a beaker so that the slide stood on one end against the wall of the beaker (Figure 1). An aqueous solution containing the protein−nanoparticle conjugates (1 nM) was introduced into the beaker dropwise using a buret or an HPLC pump. When the solution level neared the top portion of the slide, the flow was stopped and the slide rinsed with water. The portion of the slide oriented toward the bottom of the beaker remained in contact with the nanoparticle solution the longest and thus contained the highest density of particles. A constant flow created a linear density gradient across the slide. Changing the flow rate altered the slope of the gradient. Turning a 1D gradient 180 or 90° with respect to the first gradient and repeating the procedure created bidirectional and 2D protein gradients.

Exponential gradients of protein−nanoparticle conjugates could be formed using a flow rate that varied exponentially in time, or simply by using an Erlenmeyer flask instead of a beaker. Since an Erlenmeyer flask is narrower toward the top, the solution contacts the glass slide at times that increase exponentially from bottom to top.

(9) Lestelius, M.; Engquist, I.; Tengvall, P.; Chaudhury, M. K.; Liedberg, B. *Colloids Surf., B* **1999**, *15*, 57.
(10) Liedberg, B.; Tengvall, P. *Langmuir* **1995**, *11*, 3821.
(11) Liedberg, B.; Wirde, M.; Tao, Y. T.; Tengvall, P.; Gelius, U. *Langmuir* **1997**, *13*, 5329.
(12) Welin-Klintstrom, S.; Lestelius, M.; Liedberg, B.; Tengvall, P. *Colloids Surf., B* **1999**, *15*, 81.
(13) Morgenthaler, S.; Lee, S.; Zuercher, S.; Spencer, N. D. *Langmuir*, in press.
(14) Terrill, R. H.; Balss, K. M.; Zhang, Y. M.; Bohn, P. W. *J. Am. Chem. Soc.* **2000**, *122*, 988.
(15) Balss, K. M.; Coleman, B. D.; Lansford, C. H.; Haasch, R. T.; Bohn, P. W. *J. Phys. Chem. B* **2001**, *105*, 8970.
(16) Balss, K. M.; Fried, G. A.; Bohn, P. W. *J. Electrochem. Soc.* **2002**, *149*, C450.
(17) Balss, K. M.; Kuo, T. C.; Bohn, P. W. *J. Phys. Chem. B* **2003**, *107*, 994.
(18) Plummer, S. T.; Bohn, P. W. *Langmuir* **2002**, *18*, 4142.
(19) Plummer, S. T.; Wang, Q.; Bohn, P. W.; Stockton, R.; Schwartz, M. A. *Langmuir* **2003**, *19*, 7528.
(20) Fuierer, R. R.; Carroll, R. L.; Feldheim, D. L.; Gorman, C. B. *Adv. Mater.* **2002**, *14*, 154.
(21) Ruardy, T. G.; Schakenraad, J. M.; Vandermei, H. C.; Busscher, H. J. *J. Biomed. Mater. Res.* **1995**, *29*, 1415.
(22) Ruardy, T. G.; Moorlag, H. E.; Schakenraad, J. M.; VanderMei, H. C.; Busscher, H. J. *J. Colloid Interface Sci.* **1997**, *188*, 209.
(23) Daniel, S.; Chaudhury, M. K.; Chen, J. C. *Science* **2001**, *291*, 633.
(24) Daniel, S.; Chaudhury, M. K. *Langmuir* **2002**, *18*, 3404.
(25) Chaudhury, M. K.; Whitesides, G. M. *Science* **1992**, *256*, 1539.
(26) Lin, Y. S.; Hlady, V.; Janatova, J. *Biomaterials* **1992**, *13*, 497.
(27) Lin, Y. S.; Hlady, V. *Abstr. Pap. Am. Chem. Soc.* **1993**, *205*, 227.
(28) Genzer, J.; Fischer, D. A.; Efimenko, K. *Appl. Phys. Lett.* **2003**, *82*, 266.
(29) Zhao, H.; Beysens, D. *Langmuir* **1995**, *11*, 627.
(30) Walter, J.; Kernveits, B.; Huf, J.; Stolze, B.; Bonhoeffer, F. *Development* **1987**, *101*, 685.
(31) Walter, J.; Henkefahle, S.; Bonhoeffer, F. *Development* **1987**, *101*, 909.
(32) Rosentreter, S. M.; Davenport, R. W.; Loschinger, J.; Huf, J.; Jung, J. G.; Bonhoeffer, F. *J. Neurobiol.* **1998**, *37*, 541.
(33) Dertinger, S. K. W.; Jiang, X. Y.; Li, Z. Y.; Murthy, V. N.; Whitesides, G. M. *Proc. Natl. Acad. Sci. U.S.A.* **2002**, *99*, 12542.
(34) Dertinger, S. K. W.; Chiu, D. T.; Jeon, N. L.; Whitesides, G. M. *Anal. Chem.* **2001**, *73*, 1240.
(35) Grabar, K. C.; Allison, K. J.; Baker, B. E.; Bright, R. M.; Brown, K. R.; Freeman, R. G.; Fox, A. P.; Keating, C. D.; Musick, M. D.; Natan, M. J. *Langmuir* **1996**, *12*, 2353.

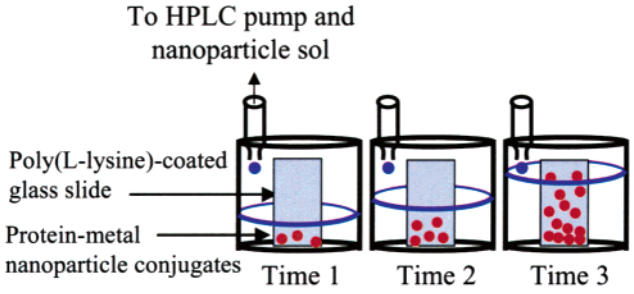

Figure 1. Schematic illustration of the formation of protein-coated metal nanoparticle gradients on solid substrates. The substrate is positioned upright along the wall of a beaker. At $t = 0$ s the flow of the nanoparticle solution into the beaker is started. With advancing time ($t > 0$ s), the beaker fills and the contact line between the solution and the substrate rises. At $t = t_{final}$ the slide is removed from the beaker and rinsed with water.

Characterization of Protein Gradients. Metal nanoparticles provide convenient handles for characterizing protein density gradients on surfaces. Once assembled onto solid supports, the density of protein−metal nanoparticle bioconjugates along the surface may be characterized with atomic force microscopy (AFM), visible absorption spectroscopy, and fluorescence microscopy. The enormous visible light extinction properties of metal nanoparticles such as gold and silver ($\epsilon > 10^8$ M^{-1} cm^{-1}) enable the determination of surface densities as low as ca. 10^8 particles cm^{-2} with visible absorption spectroscopy. Protein density along the surface can then be calculated from the number of proteins per particle (see below). Because 20 nm diameter gold and 10 nm diameter silver nanoparticles absorb visible light of different energies (λ_{max}, 525 and 400 nm, respectively), surface density gradients of two different proteins may be assembled onto a single substrate and characterized with visible absorption spectroscopy (and AFM if the particles differ in size). This type of "two-color" patterning could increase the complexity of in vitro axon guidance assays significantly. The use of protein-coated fluorescently labeled nanospheres can expand the assay to three or four colors.

Instrumentation. UV−visible spectra were acquired on a HP 8452 diode array spectrophotometer. Fluorescence spectra were acquired with a Perkin-Elmer luminescence spectrometer (LS 50B). Fluorescence microscopy images were collected with a Zeiss Axiovert 35 equipped with a Nikon color CCD camera (DXM 1200). The fluorescence images were analyzed using PaintShopPro.

Materials. All chemicals were received from the companies indicated and were used without further purification. Hydrogen tetrachloroaurate-(III) trihydrate ($HAuCl_4 \cdot 3H_2O$; Sigma), silver nitrate ($AgNO_3$; Sigma), sodium borohydride ($NaBH_4$; Sigma), poly-L-lysine hydrobromide (M_w = 4000−15 000; Sigma), (3-aminopropyl)triethoxysilane (APTES; Sigma), ephrin-A5 extracellular domain/Fc chimera (Sigma), ephrin-B1 extracellular domain/Fc chimera (Sigma), carboxylic acid-modified fluorescent latex beads (0.035 μm; Sigma), rhodamine B isothiocyanate (RB; Sigma), fluorescamine (Sigma), poly(vinylpyrrolidone) K30 (PVP, M_w = 40 000; Acros), trisodium citrate dihydrate ($Na_3C_6H_5O_7 \cdot 2H_2O$; Mallinckrodt), bis-sulfonatophosphine triphenylphosphine (BSPP; Strem), bovine serum albumin (BSA; Roche), Dulbecco's phosphate-buffered saline (DPBS buffer; Cambrex BioScience Waterville, Inc.), Dulbecco's modified eagles medium (DMEM; Cambrex BioScience), DL-dithiothreitol (TCI America), toluene (Fisher Chemicals), sulfuric acid (H_2SO_4; Fisher), hydrogen peroxide 30% (H_2O_2) (Fisher Chemicals), dimethylformamide (DMF) (Fisher Chemicals), acetone (Fisher Chemicals), ethanol absolute (Aaper Alcohol), 20 nm gold colloids (EM.GC 20, Ted Pellar, Inc.), microscopy glass slides (3 × 1 in.; Fisher), glass cover slides (22 mm × 30 mm; Electron Microscopy Science), Sephadex G-25 column (PD-10, Amersham Biosciences).

Preparation of Nanoparticles and Nanoparticle Solutions. Citrate-coated gold nanoparticles of 12 nm diameter were synthesized following the preparation by Frens.[36] Silver nanoparticles were prepared by the methods of Sun and Xia or Mirkin et al.[37−39] Gold colloids of 20 nm diameter were purchased from Ted Pella.

Preparation of Rhodamine B Isothiocyanate-Labeled BSA. RB was dissolved in dimethylformamide (DMF; 10 mg/mL), and 130 μL was immediately added to a buffered BSA solution (10 mg/mL, carbonate buffer, pH = 9) to produce a molar ratio of RB and BSA of 8:1. The mixture was incubated under continuous stirring overnight at 4 °C. After completion of the conjugation reaction a Sephadex G-25 column was used to separate the rhodamine B labeled BSA (RB-BSA) from the unreacted RB.

Preparation of Protein−Nanoparticle Conjugates. All protein−gold nanoparticle conjugates were prepared in a similar fashion. For example, in the preparation of BSA and RB-BSA gold nanoparticle conjugates, 1.05 nmol of protein was mixed with 0.1 mL of 10 mM phosphate buffer (pH = 7.4). The protein solution was added to 0.9 mL of 20 nm gold nanoparticles (1.16 nM) to achieve a ratio of ~1000 protein molecules/(gold nanoparticle). The mixture was incubated on a shaker for 30 min. The solution was then centrifuged at 13 000 rpm for 30 min to separate the unbound proteins from the conjugates. The supernatant containing unbound proteins was removed carefully, and the pellet was resuspended in phosphate buffer (10 mM, pH = 7.4).

Ephrin-A5 or ephrin-B1 gold nanoparticle complexes were prepared by mixing the proteins (10.5 pmol ephrin-A5 or 26.2 pmol ephrin-B1, respectively) with 0.05 mL of 10 mM carbonate buffer (pH = 11) and adding the protein solution to 0.45 mL of 20 nm gold nanoparticles (1.16 nM) in protein nanoparticle ratios of 20:1 and 50:1, respectively. After 10 h incubation time the unbound proteins and the protein−particle conjugates were separated by centrifugation at 8500 rpm for 30 min. The conjugates were resuspended in 10 mM carbonate buffer (pH = 11).

Quantifying Proteins on Gold Nanoparticles Using Fluorescamine. To determine the number of ephrine-A5 and ephrine-B1 proteins bound per nanoparticle, the fluorescamine assay was used. Fluorescamine (4-phenylspiro[furan-2(3*H*),1-phthalan]-3,3′-dione) is a non-fluorescent molecule which reacts rapidly and in high yield with primary amines in proteins to form a highly fluorescent pyrrolinone moiety.

Fluorescamine assays were performed by preparing five standards, each with a volume of 1.5 mL, in pH 11 carbonate buffer. For ephrine-A5 the concentrations varied from 0 to 8.17 nM, and for ephrine-B1 the concentrations ranged from 0 to 17.8 nM. A 0.5 mL aliquot of fluorescamine solution (1.08 mM in acetone) was added to each of the standard solutions and mixed for 5 min. The intensities of the solutions were measured and plotted vs protein concentration to generate a standard curve.

The number of protein molecules bound per gold nanoparticle was determined by a difference measurement. Ephrin-A5 and ephrin-B1 gold nanoparticle conjugates were prepared and centrifuged to remove the unbound protein. The supernatants were subjected to the fluorescamine assay. The supernatants were diluted to 1.5 mL with pH 11 carbonate buffer and then mixed with 0.5 mL of 1.08 mM fluorescamine in acetone for 5 min. The amount of unbound protein in the supernatant was determined by comparing the intensities of the samples to the standard curve. The number of proteins attached to the gold particles was calculated by subtracting the amount of free protein, as determined by the fluorescence measurement, from the total amount of protein added initially.

Preparation of Substrates. Glass substrates were cleaned by immersion into piranha solution (H_2SO_4:H_2O_2 (30%), 3:1) (*CAUTION*: Piranha solution is a strong oxidizer and reacts violently with any organic material. It should be handled only in small volumes and

(36) Frens, G. *Nature (London), Phys. Sci.* **1973**, *241*, 20.
(37) Jin, R. C.; Cao, Y. W.; Mirkin, C. A.; Kelly, K. L.; Schatz, G. C.; Zheng, J. G. *Science* **2001**, *294*, 1901.
(38) Jin, R. C.; Cao, Y. C.; Hao, E. C.; Metraux, G. S.; Schatz, G. C.; Mirkin, C. A. *Nature (London)* **2003**, *425*, 487.
(39) Sun, Y. G.; Xia, Y. N. *Science* **2002**, *298*, 2176.

with extreme care) for 15 min, followed by thorough rinsing with DI water and drying in a stream of N_2.

Glass slides were silanized in 35 mL of dry toluene (freshly distilled) with 100 μL of (aminopropyl)triethoxysilane (APTES) for 15 min, rinsed with toluene, sonicated for 10 min in toluene, rinsed with ethanol, sonicated for 10 min in ethanol, and finally dried in a stream of N_2.

Poly-L-lysine solutions were prepared by dissolving 0.35 mg/mL of poly-L-lysine hydrobromide in DPBS buffer. The clean glass slides were immersed into the poly-L-lysine solution overnight, rinsed with DI water, and dried in a stream of N_2. All poly-L-lysine-coated slides were used directly after drying. Prolonged storage of the slides in air led to failure in the deposition of nanoparticles.

Nanoparticle-surface adsorption vs time transients were measured by immersing the substrate into a particle solution for a predetermined amount of time, rinsing it with DI water, and placing it in a water-filled UV−visible cuvette, where an absorbance spectrum was measured. The sample was then reimmersed into the nanoparticle solution until the next measurement.

Growth of Hippocampal Cells on Nano-gold Slides. Hippocampal neurons were harvested from embryonic day 18 rat tissue as described previously and plated at 9.5×10^3 cells/cm^2.[40] Growth was photographed using a Nikon cool-pix camera after 5 days in culture. For immunostaining, cells were fixed in 4% paraformaldehyde plus 0.1% Triton X-100, washed two times in PBS and blocked with PBS + 3% goat serum (blocking buffer). Rabbit anti-goat MAP2 antibody (Santa Cruz Biotech, Santa Cruz, CA) was added at a dilution of 1/1000, incubated at 4 °C overnight, and washed 3 times with blocking buffer. TRITC-conjugated anti-goat secondary antibody (molecular probes, Eugene, OR) was added at 1/1000 dilution, incubated for 2 h at room temperature, and washed 3 times in PBS. Cells were plated onto coverslips, and MAP2 staining was visualized with a fluorescence microscope.

Results and Discussion

Metal Nanoparticle Gradients. Colloidal metal particles are kinetically stable suspensions of nanometer-sized metals. They are typically synthesized via aqueous procedures in which a metal precursor complex is reacted with a chemical reducing agent. A classic procedure for producing gold nanoparticles involves the reduction of hydrogen tetrachloroaurate(III) by trisodium citrate in aqueous solution.[36,41−43] The preparation yields gold particles whose diameters are determined largely by the initial citrate:$[AuCl_4]^-$ stoichiometry. Particles with diameters from 2 to 200 nm with <10% size disparity can be made with this procedure.

The stability of colloidal solutions is due to a balance of forces including electrostatic repulsion, van der Waals attraction, and mixing free energy.[44] The former two forces have been condensed into the well-known DLVO theory (so named for its creators Derjaguin, Landau, Verwey, and Overbeek) that explains the stability of charged particles. In DLVO theory, the attraction between two spheres, due to their polarizability (van der Waals attraction), is compensated for by repulsive forces acting between the electrical double layers of the two spheres. Specifically, the electrostatic repulsion varies as r^{-1}, while the van der Waals attraction has an r^{-3} dependence, where r is separation distance. Thus, the electrical double layer normally prevents charged particles from approaching each other to within distances where their van der Waals attraction can pull them together. The citrate reduction method produces negatively charged colloidal gold particles, an important consideration when preparing protein−gold conjugates or gold particle-modified substrates.

Gold nanoparticles are negatively charged due to adsorbed citrate and chloride ions while the free amine groups of the poly-L-lysine layer are positively charged at the pH of the aqueous nanoparticle suspension. These opposite charges lead to electrostatic attraction, resulting in the binding of the nanoparticles to the substrate. Rather than dipping the slides into the nanoparticle solution at a defined speed, which requires a mechanical device, we have chosen to fill a beaker containing the substrate at a constant and controlled flow rate with the nanoparticle solution. The flow rate determines the time the substrate is in contact with the nanoparticle solution and therefore controls the amount of particles that bind to the substrate. Figure 1 shows this procedure schematically. Figure 2A shows as an example the UV−visible absorbance spectra of a poly-L-lysine-coated glass slide after the formation of a gold nanoparticle gradient (no protein was used in this example). The maximum time for the adsorption was 15 min. The top spectrum was collected on the high-density side of the gradient (longest adsorption time), and the slide was shifted 0.25 cm for each consecutive spectral measurement. The absorbance value of the surface plasmon band varied continuously along the surface. Grabar et al. related the UV−visible absorbance values with the number density of particles on the surface and determined the extinction coefficient for 10 nm gold particles on a surface.[45] Figure 2B shows the measured absorbance values

$$\Gamma = \frac{N_A A}{2 \times 1000\epsilon}$$

at 520 nm (on the left axis) and the calculated particle density (on the right axis) versus the distance along the slide. The number of particles per unit area increased linearly across the slide.

The adsorption kinetics of metal nanoparticles onto glass slides are important in the preparation of density gradients. If adsorption kinetics are too fast, it is difficult to control gradient slope because the difference in the number of particles adsorbed along the length of the slide will be small. Nanoparticle adsorption transients were measured by UV−visible absorption spectroscopy for three different types of nanoparticles, citrate-capped gold nanoparticles, BSPP-capped silver nanoparticles (BSPP is bis(sulfonatophenyl)phenylphosphine) and PVP-capped silver nanoparticles (PVP is poly(vinylpyrrolidone)). Despite the different capping agents, the shapes of the kinetic curves remained the same (Supporting Information). At the beginning of the transient, a roughly linear increase in absorbance vs time was observed. The absorbance leveled off to a constant value, which represents the maximum amount of particles adsorbed to the surface. The slope of the linear part of the curves is strongly dependent upon particle type and concentration. Lower concentrations and larger nanoparticles

(40) Osten, P.; Srivastava, S.; Imman, G. J.; Vilim, F. S.; Kharti, L.; Lee, L. M.; States, B. A.; Einheber, S.; Milner, T. A.; Hanson, P. I.; Ziff, E. B. *Neuron* **1998**, *21*, 99.
(41) Frens, G. *Kolloid-Z. Z. Polym.* **1972**, *250*, 736.
(42) Keating, C. D.; Kovaleski, K. M.; Natan, M. J. *J. Phys. Chem. B* **1998**, *102*, 9404.
(43) Keating, C. D.; Musick, M. D.; Keefe, M. H.; Natan, M. J. *J. Chem. Educ.* **1999**, *76*, 949.
(44) Hunter, R. J. *Foundations of Colloid Science*, 2nd ed.; Oxford University Press: Oxford, U.K., 2001.
(45) Grabar, K. C.; Smith, P. C.; Musick, M. D.; Davis, J. A.; Walter, D. G.; Jackson, M. A.; Guthrie, A. P.; Natan, M. J. *J. Am. Chem. Soc.* **1996**, *118*, 1148.

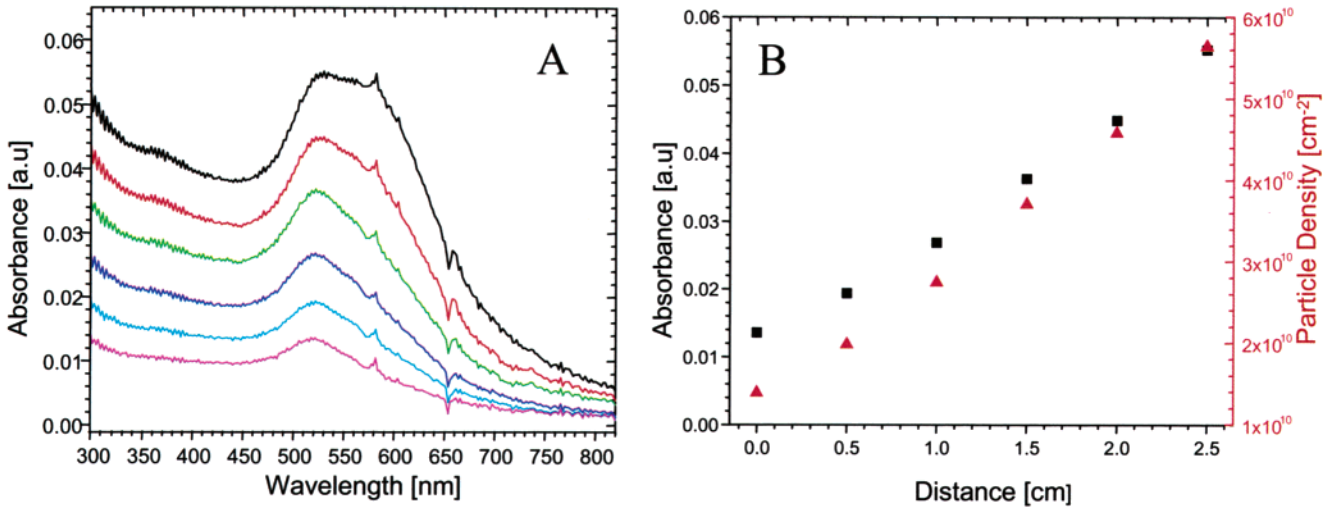

Figure 2. (A) UV−visible absorption spectra of a gradient of citrate-coated gold nanoparticles adsorbed onto a poly-L-lysine substrate. Each spectrum was taken at a different position on the substrate. The lowest intensity spectrum was acquired on the low-density side of the rectangular slide (arbitrarily assigned as "0 cm"), and the slide was translated a distance of 0.25 cm for each subsequent spectrum. (B) Plot of the absorbance values at the peak maximum versus the distance along the gradient axis. The left axis presents the absorbance of the plasmon band (black squares), and the right axis is the calculated nanoparticle density (red circles). Gold nanoparticle concentration was 30 nM.

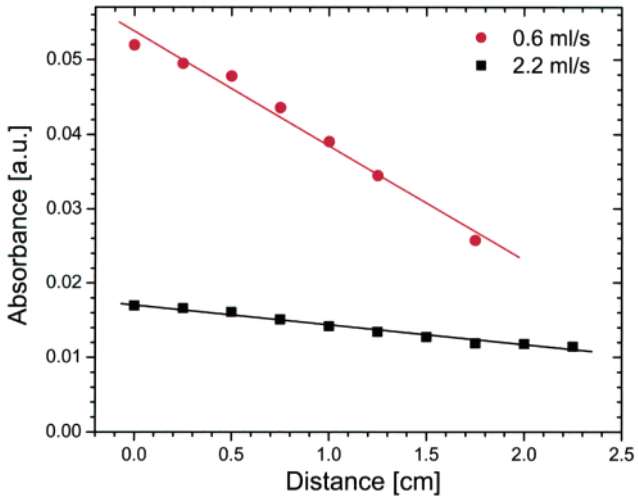

Figure 3. Absorbance vs distance plots of citrate-capped gold nanoparticle gradients prepared with different flow rates: (circles) 0.6 mL/s; (squares) 2.2 mL/s. Substrate was poly-L-lysine-terminated glass.

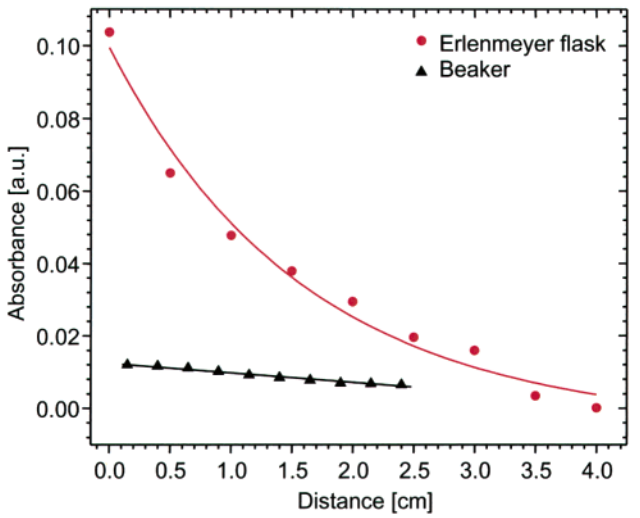

Figure 4. Absorbance vs distance plots of citrate-capped gold nanoparticle gradients prepared on poly-L-lysine-coated substrates in a cylindrical vial (black triangles) and in an Erlenmeyer flask (red circles).

resulted in slower adsorption kinetics (data not shown). These kinetic plots give a rough idea of the time needed to prepare a surface gradient and the range of particle densities possible using this method. To achieve a linear gradient an adsorption time in the linear regime of the transient should be chosen. To remain in the linear regime of the adsorption transient, the total time to assemble a linear density gradient was kept below 15 min. Within this constraint, changes in the flow rate lead directly to a change in the amount of particles adsorbed onto the substrate and in turn a change in the slope of the gradient. Figure 3 shows that the slope of the gradient changes by roughly a factor of 6 when flow rate is changed from 0.6 to 2.2 mL/s.

Exponential gradients are also possible with this method. Perhaps the simplest means of varying the fill rate in exponential fashion is to use an Erlenmeyer flask instead of a cylindrical beaker. The Erlenmeyer flask is conical with a larger diameter at the bottom and a smaller diameter at the neck. If the flask is filled at a constant flow rate from a pump or buret, the rise in the liquid level is nonlinear in time. In Figure 4 the difference between gradients prepared in a cylindrical beaker vs an Erlenmeyer flask is shown. The beaker resulted in a linear gradient, while the Erlenmeyer flask gave a nonlinear shape, which could be fit to an exponential decay.

When preparing substrates for axon guidance assays, it is important to be able to form multiprotein gradients (of chemoattractants and chemorepellants, for example) in which the density of each protein can be determined independently. The use of silver and gold nanoparticles enables the simultaneous determination of multicomponent gradients. Visible absorption spectroscopy data for a bidirectional gradient made with silver and gold nanoparticles is shown in Figure 5. The intensity of the absorbance maximum for the peak of the silver nanoparticles decreased across the slide, while that for the gold nanoparticle peak increased. We have also assembled 2D gradients using protocols similar to those reported by Natan (see Supporting Information).

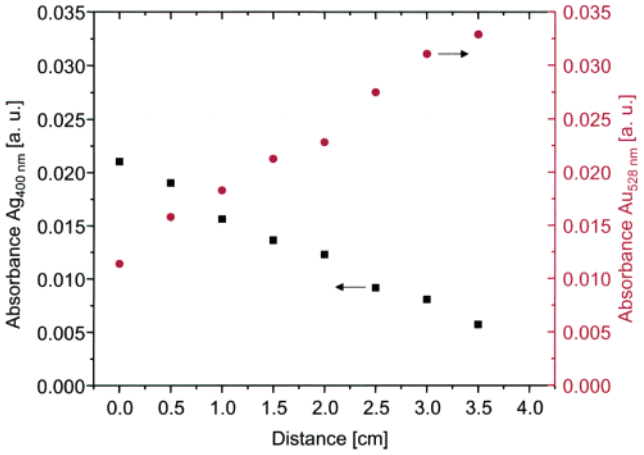

Figure 5. Visible light absorbance vs distance plots of a bidirectional gradient. The left axis (black squares) is the absorbance of silver nanoparticles across the slide (peak at ca. 400 nm), and the right axis is the absorbance of gold nanoparticles (peak at 528 nm).

The preparation of nanoparticle gradients as described above is not limited to metal nanoparticles. Gradients were also fabricated with carboxylic acid-modified latex beads. The latex beads are commercially available in different sizes and with a number of fluorescent labels, opening a variety of possibilities for three- or four-color (protein) density gradients. Gradients of latex beads were prepared as described for metal nanoparticles. Fluorescence microscopy images show a decrease in fluorescence intensity along the length of the gradient starting from high coverage to low coverage (Figure 6A). With the help of imaging analysis software, it was possible to determine quantitatively the fluorescence emission intensity of the images. Figure 6B shows that the gradient has a linear slope as observed for the metal nanoparticle gradients.

Protein−Metal Nanoparticle Gradients. Surface-bound protein gradients can be prepared with protein−metal nanoparticle conjugates using the methods described above. For example, BSA, ephrine-A5, and ephrin-B1 gold nanoparticle conjugates were prepared, and the number of proteins per nanoparticle was determined to be 160 ± 6, 15 ± 1, and 40 ± 2, respectively (deviations were based on three measurements).[46] Figure 7 reveals that the conjugates formed gradients much like the citrate-coated gold and BSPP-coated silver nanoparticles. Two experiments were performed in order to show that the protein was still bound to the gold nanoparticles after adsorption to the surface. First, BSA was modified with the fluorescent molecule rhodamine B-isothiocyanate (RB-BSA) and conjugated to gold nanoparticles. These particles were used to prepare a RB-BSA gradient. UV−visible absorption spectra confirmed the presence of a gold nanoparticle gradient on the surface. The fluorescence of RB-BSA conjugated to gold nanoparticles was then detected by fluorescence microscopy. The emission intensity of the substrate changed when the position of the measurement along the axis of the gradient was altered. Figure 8A shows fluorescence images at four different positions along the gradient. The emission intensity decreased as the density

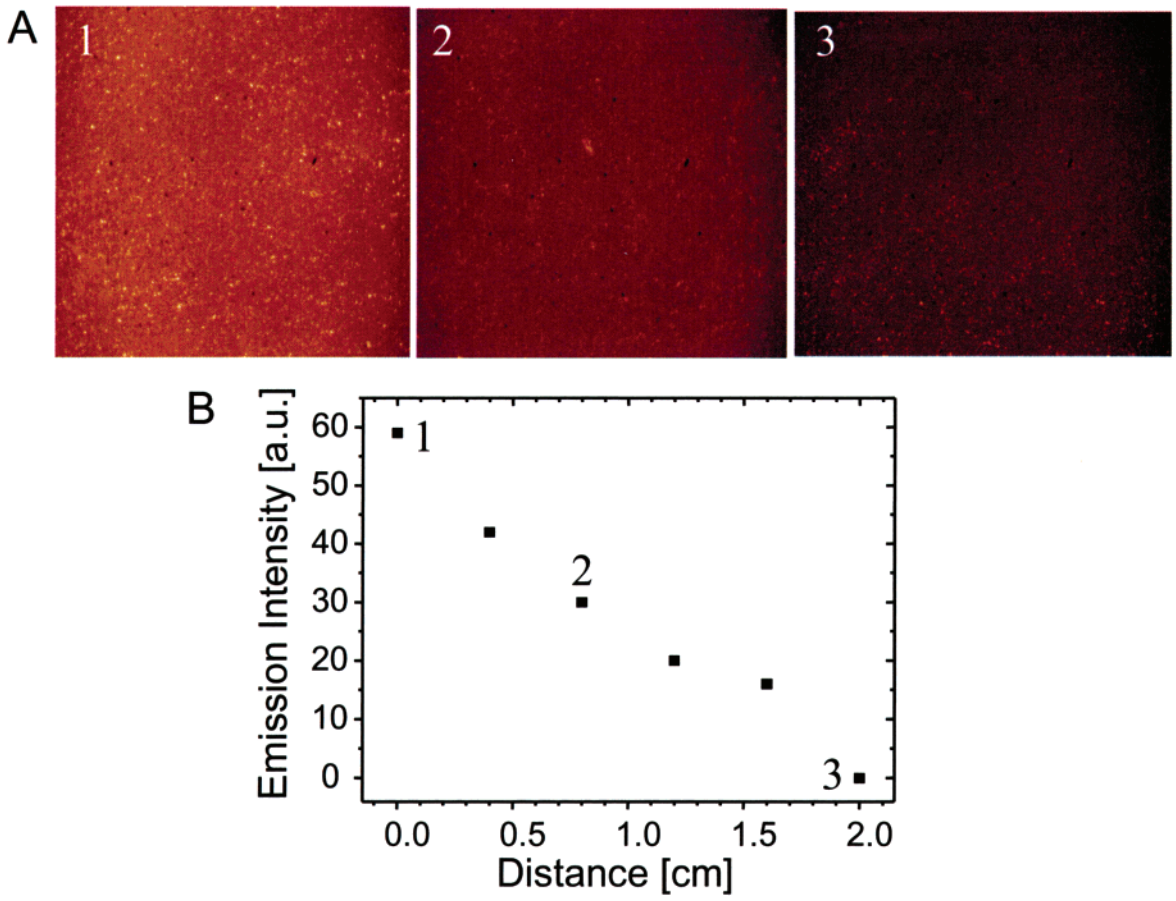

Figure 6. (A) Fluorescence microscopy images of a gradient prepared by the adsorption of carboxylic acid-modified fluorescence latex beads onto a poly-L-lysine substrate. The images are taken at different regions along the axis of the gradient. Each image is 670 μm × 535 μm. (B) Intensity values vs distance plot of the gradient shown in A. The points numbered in B correspond to the images numbered in A.

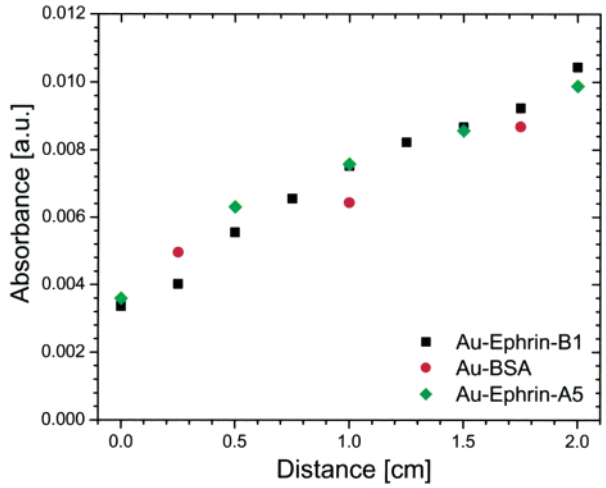

Figure 7. Absorbance vs distance plot of three different protein−gold nanoparticle conjugate gradients on poly-L-lysine substrates: (squares) ephrin-B1; (circles) BSA; (diamonds) ephrin-A5. Protein−gold nanoparticle conjugate concentrations were 1 nM.

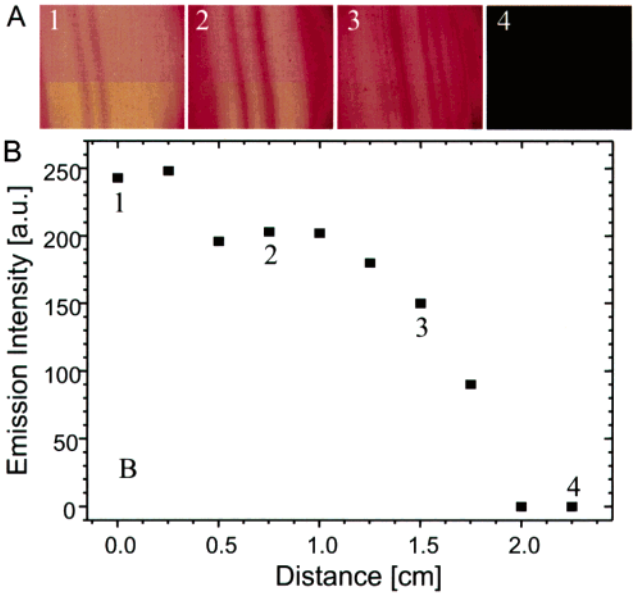

Figure 8. (A) Fluorescence microscopy images of a gradient prepared by the adsorption of RB-BSA−gold nanoparticle conjugates. Each image is 670 μm × 535 μm. (B) Intensity vs distance plot of the gradient shown in A. (Vertical striping results from scratching during sample mounting.) The points numbered in B correspond to the images numbered in A.

of gold nanoparticles decreased. When the peak position was plotted vs distance across the slide, the shape and slope of the protein gradient was apparent (Figure 8B).

Additional evidence that proteins remained bound to the gold nanoparticles after adsorption to the substrate was obtained by removing the proteins via ligand exchange. Thiol-terminated molecules can replace ligands bound to gold nanoparticles.[47,48] Therefore, it was expected that an alkanethiol ligand would transfer the rhodamine B-labeled BSA molecules from the substrate into solution where they could be detected by fluorescence spectroscopy. The water-soluble dithiothreitol (DTT) was chosen to replace the surface-bound protein because it is soluble in high concentrations in water. After binding RB-BSA−gold nanoparticle conjugates to a poly-L-lysine slide (with homogeneous density distribution), the sample was immersed for 2 days in an aqueous solution of 0.1 M DTT. Freshly prepared DTT solution is not fluorescent. The fluorescence spectrum of the DTT solution that was in contact with the RB-BSA gold nanoparticle substrate revealed an emission peak around 600 nm, which is characteristic of rhodamine B isothiocyanate (Supporting Information). The data indicate that RB-BSA remained bound to gold nanoparticles following adsorption to the substrate and suggest that a quantitative relationship exists between nanoparticle coverage and protein density. Because nanoparticle coverage is obtained easily and sensitively with simple UV−visible absorption spectroscopy, metal nanoparticles are effective optical tags for characterizing protein density gradients.

Axon Growth on Protein−Metal Nanoparticle-Coated Substrates. Finally, protein−metal nanoparticle-coated substrates were tested for their compatibility with neurons. A number of substrate coatings were used—poly(4-vinylpyridine), APTES, poly-l-lysine—and the latter was found to be the only one which supported growth of embryonic rat hippocampal neurons. Hippocampal neurons were then cultured on poly-L-lysine slides covered with protein−gold nanoparticle conjugates. We find that hippocampal neurons, cultured for 5 days in vitro atop BSA−gold nanoparticle slides remain healthy and extend multiple neurites in culture (Figure 9A). To test whether hippocampal cells grown on nanoparticle-coated slides express specific neuronal markers, we stained hippocampal cultures grown on BSA−gold nanoparticle slides for the dendritic marker MAP2 (Figure 9B). We find that MAP2 is expressed and localizes normally in hippocampal cells grown on BSA−gold nanoparticle-coated substrates. Thus, the presence of gold nanoparticles does not have a deleterious effect on nerve cell growth. To test whether the protein−nanoparticle conjugates were functional after placement on glass slides, we plated rat neonatal hippocampal neurons onto slides fabricated with gold nanoparticles carrying the axon repellent, ephrin-A5. Hippocampal neurons express multiple receptors for ephrin-A5 on their axons and dendrites. After 9 days in vitro, cells plated on ephrin-A5 slides exhibit significantly less neurite outgrowth and branching compared to slides coated with BSA−gold nanoparticle conjugates (Figure 9C), consistent with ephrin-A5 remaining active after the gold conjugation procedure.

In its current form, the nanoparticle gradient fabrication method described above is appealing because of its simplicity and versatility. There is a caveat, however, when using these gradients in solutions of high ionic strength such as cellular growth media for extended periods of time. As Figure 10 shows, a fraction of the protein−metal nanoparticle bioconjugates will desorb from the surface over time when placed in high ionic strength solutions (17% loss in 48 h). This is a result of the relatively labile electrostatic interactions holding the protein−metal nanoparticle conjugate to the surface. We are currently addressing this problem through the use of a more robust covalent linkage between nanoparticles and poly-L-lysine-coated slides.

(46) Xie, H.; Tkachenko, A. G.; Glomm, W. R.; Ryan, J. A.; Brennaman, M. K.; Papanikolas, J. M.; Franzen, S.; Feldheim, D. L. *Anal. Chem.* **2003**, *75*, 5797.
(47) Hostetler, M. J.; Templeton, A. C.; Murray, R. W. *Langmuir* **1999**, *15*, 3782.
(48) Song, Y.; Murray, R. W. *J. Am. Chem. Soc.* **2002**, *124*, 7096.

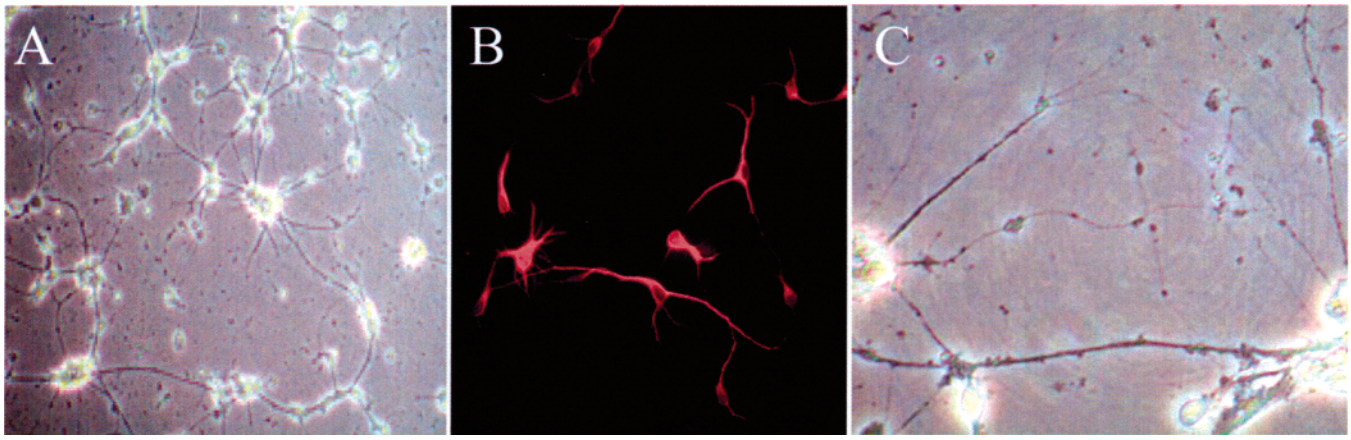

Figure 9. Rat hippocampal neurons grow, send out neural processes, and localize endogenous proteins when grown on nanoparticle-coated slides. (A) Embryonic day 18 (E18) rat hippocampal cells were harvested and plated on slides coated with BSA-coated gold nanoparticles. After 5 days in culture many neurites can be seen growing out from the cell bodies. (B) MAP2 is expressed and localized normally in hippocampal cultures grown on BSA−gold nanoparticle-coated slides. E18 hippocampal cells were plated on slides coated with BSA-coupled nanoparticles and allowed to grow out over 5 days in culture. MAP2 was detected using indirect immunoflourescence and is localized to dendrites in these cells. (C) Rat hippocampal cells plated on slides coated with ephrin-A5−gold nanoparticle conjugates. Active ephrin-A5 does not support the extension of neurites.

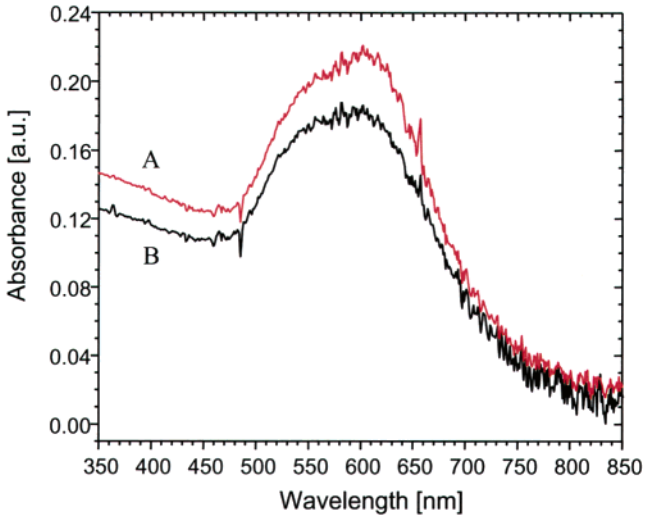

Figure 10. UV−visible spectra for an RB-BSA−gold nanoparticle-coated slide prior to (A) and following (B) immersion in Dulbecco's modified eagles medium (DMEM) growth media for 48 h.

Conclusions

The goal of this work was to develop a method for creating protein density gradients on solid supports for studies of neural growth and axon guidance. We sought a method that is versatile, rapid, and routine. Ideally, the method would be compatible with any substrate material, capable of forming molecular gradients of any desired concentration and slope, and in two dimensions, and would not involve expensive or sophisticated equipment. We have shown that nanometer-scale metals are well-suited for this application because they may be modified with nearly any protein or protein receptor, adsorb to surfaces in patterns determined simply by immersion time, and are exceptionally sensitive optical tags. The utility of the method was demonstrated by creating gradients of axon guidance molecules on cover slips and showing that the substrates affect axon and dendrite extension. Our future work will focus on the effects of gradient slope, shape, and composition (e.g., bidirectional gradients of chemoattractants and chemorepellants) on axon guidance. However, the method in principle could be used for any biological inquiry where gradients of molecules are important for cellular function.

Acknowledgment. D.L.F. thanks the David and Lucile Packard Foundation, NIH, and NSF for partial support of this work. D.A.F. thanks Lindsay Hinck, Will McKenna, and Alexa Maksimova for assistance with the hippocampal cultures.

Supporting Information Available: Experimental figures (PDF). This material is available free of charge via the Internet at http://pubs.acs.org.

JA031674N